Journal of Metals, Materials and Minerals, 34(1), 1910, 2024

In vitro and vivo biocompatibility and degradability of low-alloyed Mg-Zn-Ca-MgO composite as bone repair biomaterials

Shuquan ZHANG[1,2,3,*], Jiangtao FENG[1,2,3], Chaokun TANG[4], Ran PANG[1,2,3], Xinglong ZHANG[1,2,3], Chenguang LI[1,2,3], Weihao ZHANG[1,2,3], Fengxin ZHOU[1,2,3], Feng XUE[1,2,3], Shaoyuan LYU[4], Minfang CHEN[4,5,6], and Hao WANG[7]

[1] *Department of Orthopedics, Integrated Chinese and Western Medicine Hospital, Tianjin University, Tianjin, 300072, China*
[2] *Department of Orthopedics, Tianjin Hospital of Integrated Chinese and Western Medicine, Tianjin, 300100, China*
[3] *Department of Orthopedics, Tianjin NanKai Hospital, Tianjin, 300100, China*
[4] *School of Materials Science and Engineering, Tianjin University of Technology, Tianjin, 300384, China*
[5] *National Demonstration Center for Experimental Function Materials Education, Tianjin, 300384, China*
[6] *Key Laboratory of Display Materials and Photoelectric Device (Ministry of Education), Tianjin, 300384, China*
[7] *Medical School of Tianjin University, Tianjin University, Tianjin, 300072, China*

***Corresponding author e-mail**: zhangshuquan666@126.com

Received date:
7 December 2023
Revised date
7 January 2024
Accepted date:
11 January 2024

Keywords:
Magnesium alloys;
Bone regeneration;
Cell-compatibility;
Corrosion

Abstract

Magnesium alloys have gained attention as biodegradable bone repair biomaterials. Unlike non-biodegradable materials like titanium and tantalum, biodegradable implants offer advantages in promoting bone healing and minimizing chronic inflammatory reactions. However, the impact of the implant's degradation on the osteogenic environment remains a concern. The Mg-Zn-Ca-MgO composite, being biocompatible and containing osteogenic ions, is a promising candidate. This study assesses the degradability and in vitro/in vivo biocompatibility of two Mg-Zn-Ca-MgO composites with varying degradation rates. The Mg-1Zn-0.2Ca-1.0MgO composite was prepared, and leaching solutions were created following standard protocols. MC3T3-E1 cell cultures were conducted to assess cell toxicity, alkaline phosphatase (ALP) staining, cytoskeleton morphology, and osteogenic protein expression. In vivo biodegradation and bone regeneration capacity were evaluated in rat femoral condyles. Benefiting from the more protective corrosion product layer on the surface, the ultra-fine grained (UFG) composite showed better corrosion resistance and lower Mg^{2+} release than the coarse-grained (CG) composite. UFG material exhibited higher cell viability, cytoskeleton integrity, ALP secretion, and osteogenic protein expression. In vivo, UFG composites led to greater bone regeneration and exhibited excellent biocompatibility. The UFG Mg-Zn-Ca-MgO composite demonstrates enhanced biocompatibility, corrosion resistance, and bone regeneration potential. This study highlights the importance of controlling Mg ion release for optimal bone healing in biodegradable materials.

1. Introduction

Magnesium alloy, as a biodegradable bone repair biomaterials that has been widely studied in recent years, has a broad application prospect in the fields of internal fixation of fractures and repair of bone defects [1-3]. Unlike titanium, tantalum, and polyetheretherketone (PEEK), which are extensively employed, biodegradable implants can enhance the bone healing process and are gradually assimilated by the body following the regeneration of damaged bone tissue, thus mitigating the risk of chronic inflammatory reactions associated with long-term implant presence [4]. Nevertheless, due to their degradability, the impact of the implant's degradation process on the surrounding osteogenic environment must also be considered.

Mg-Zn-Ca-MgO composite exhibits excellent biocompatibility as it consists solely of elements essential for the human body. Furthermore, the degradation products contain trace amounts of Mg^{2+}, Zn^{2+}, and Ca^{2+} ions, which can be absorbed by the body and possess osteogenic properties [5]. However, it has been shown that excess magnesium ions may inhibit cell growth [6]. Therefore, for materials with varying degradation rates, it is imperative to investigate their ion release at different concentrations as well as their in vitro and in vivo biocompatibility. On this basis, the present study focused on the degradability and in vitro and in vivo biocompatibility of two Mg-Zn-Ca-MgO composite with different degradation rates.

2. Material and methods

2.1 Materials preparation

In this study, the Mg-1Zn-0.2Ca-1.0MgO composite used was fabricated by combining high-purity Mg (99.99 wt%), Zn (99.99 wt%), and Mg-25Ca (wt%) master alloys at 780°C in an inert gas atmosphere consisting of N_2 and SF_6. MgO nanoparticles (MgO NPs) were preheated to 200°C in a muffle furnace and then introduced into the melt at 780°C using a high-shear stirrer and ultrasonic treatment [7]. The molten mixture was cast into a cylindrical ingot with a diameter of 60 mm. After homogenization at 420°C for 8 h, the extrusion process was performed at 270°C to produce material with ultra-fine grains (referred to as UFG) and at 330°C to yield material with coarse grains (referred to as CG). An extrusion ratio of 56 was used to obtain rods with a diameter of 8 mm. Test specimens were subsequently obtained by cutting the extruded rods.

2.2 Leaching solution preparation

Leaching solutions for the UFG and CG composites were prepared following ISO 10993-5 and ISO 10993-12 protocols. The α-minimum essential medium (α-MEM), a selected cell culture fluid, was chosen as the leaching medium. A ratio of 1.25:1 between the sample surface area (cm^2) and the α-MEM volume (mL) was selected to ensure efficient extraction.

Using specialized 15 mL centrifuge tubes for the specimens, the specimens were introduced, and the tubes were filled with an equal volume of α-MEM cell culture fluid. The tubes were then positioned in a controlled cell culture environment for precisely 24 h, resulting in a leaching solution with a 100% pure concentration.

To perform a comprehensive assessment, the leaching solution was diluted using α-MEM cell culture fluid to achieve concentrations of 0% and 25%. The 0% concentration served as a control, consisting only of pure α-MEM cell culture fluid without any magnesium leaching solution.

2.3 Revival and culturing of MC3T3-E1 cells

Pre-warm a water bath to 37°C, rapidly transfer the frozen cells to the bath for quick thawing, and then place them within a sterile laminar flow cabinet. Centrifuge the cells to generate a suspension, distribute them into culture bottles, and carefully introduce α-MEM culture medium. Label the bottles and place them in an incubator.

2.4 Cell toxicity assessment

Cultured actively proliferating cells were selected and seeded into a 96-well cell culture plate. The introduced leaching medium filled the seeded wells, with each group having triplicate wells. Cell viability, determined through CCK-8 assays, was assessed on days 1, 3, and 5. Optical density (OD) values were measured employing an enzyme-linked immunosorbent assay (ELISA) reader, enabling calculation of the relative cell growth rate.

2.5 Alkaline phosphatase (ALP) staining

After co-cultivating MC3T3-E1 cells with magnesium alloy leaching medium for 7 days, the cells were fixed using tissue cell fixative. Subsequently, pre-prepared ALP staining solution was added after washing, and the samples were incubated in darkness for 15 min. Next, the samples were washed and subjected to a 3 min counterstaining using Nuclear Fast Red staining solution. The stained samples were subsequently examined under a microscope.

2.6 Cell cytoskeleton and nucleus staining

Following 48 h of cultivation, cell cytoskeleton visualization was conducted through phalloidin-based staining, with 4',6-diamidino-2-phenylindole (DAPI) staining applied to label cell nuclei. These two stains were excited using separate wavelengths: phalloidin was excited at 488 nm, and DAPI at 340 nm.

2.7 Western blot for osteogenic protein expression

Following a 7-day co-culture, cells were harvested, lysed, and protein concentration was assessed. The samples underwent electrophoresis, membrane transfer, and blocking. Primary antibodies including bone morphogenetic protein 2 (BMP-2), Collagen I (Col-1), osteopontin (OPN), and runt-related transcription factor 2 (Runx2) were applied overnight (1:1000), followed by secondary antibodies (1:10,000) for 2 h. Chemiluminescence was detected subsequent to washing. Band intensities and molecular weights were analyzed after scanning.

3. Results and discussion

Figure 1(a) and Figure 1(b) show the grain structure of UFG and CG composites. The results indicate that the UFG composite exhibits a distinct bimodal structure, consisting of fully dynamically recrystallized (DRXed) regions and un-dynamically recrystallized (un-DRXed) regions. The average grain size of DRXed region is 0.49 μm. However, the average grain size of CG composite is 7μm despite owing a fully dynamic recrystallized structure. The release of Mg^{2+} ion at different times post-extraction and the corresponding annual corrosion rates are shown in Figure 1(c) and Figure 1(d). As it shows in the result, both materials show a progressively decreased corrosion rate with increase of extraction times. This is related to the formation of a protective corrosion product layer on the surface of the composite during extraction process. It is noteworthy that the Mg^{2+} ion release from the UFG composites was significantly reduced after 144 h of extraction. The average corrosion rate of UFG composites is 0.5 $mm{\cdot}y^{-1}$ ± 0.07 $mm{\cdot}y^{-1}$, which is lower than that of CG composite (0.59 $mm{\cdot}y^{-1}$ ± 0.09 $mm{\cdot}y^{-1}$) and shows better corrosion resistance, as calculated by ion release.

Figure 2(a) illustrates the results of in vitro cytoskeleton staining experiments. The nucleus is labelled in blue and the protein skeleton is labelled in red by F-actin dye. From the results, the number of surviving cells in the UFG composite group is much higher than that in the CG composite group. At the same time, from the cell nucleus and cytoskeleton combination diagram, the protein skeleton around the nucleus of UFG composite can basically fill the whole cell and has a densely distributed. The cells exhibited a levelled polygonal morphology with extensions of cytoplasm in diverse directions, which displayed normal cell cytoskeleton morphology [8]. It showed good growth state of MC3T3-E1 cells. The following cytotoxicity experiment (CCK-8) in Figure 2(b) also obtained a similar result.

From the OD value at 450 nm, the total number of cells in the UFG and CG composites showed an increasing trend. Where the OD value of UFG composite after 1, 3 and 5 days of culturing was slightly higher than that of the control group. But the OD value of CG was significantly lower than that of control group at day 3 and 5. Therefore, in terms of cell survival rate, the cell viability of both materials was greater than 100% at 1 day of co-culture, and CG possessed a significantly higher cell survival rate. While at time 3 and 5 days of co-culture, the cell survival rate of CG composite material group gradually decreased. This suggests that the value-added and differentiation of MC3T3-E1 may be negatively affected under higher concentrations of magnesium ions. In contrast, the UFG composites group consistently maintained a cell survival rate of over 100%.

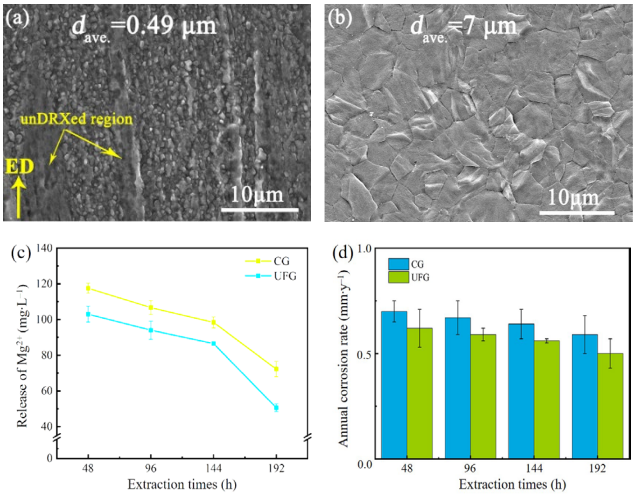

Figure 1. SEM images of UFG (a) and CG (b), Mg^{2+} ion release in Magnesium ion release in α-MEM (c), and average corrosion rate calculated by Mg^{2+} ion release.

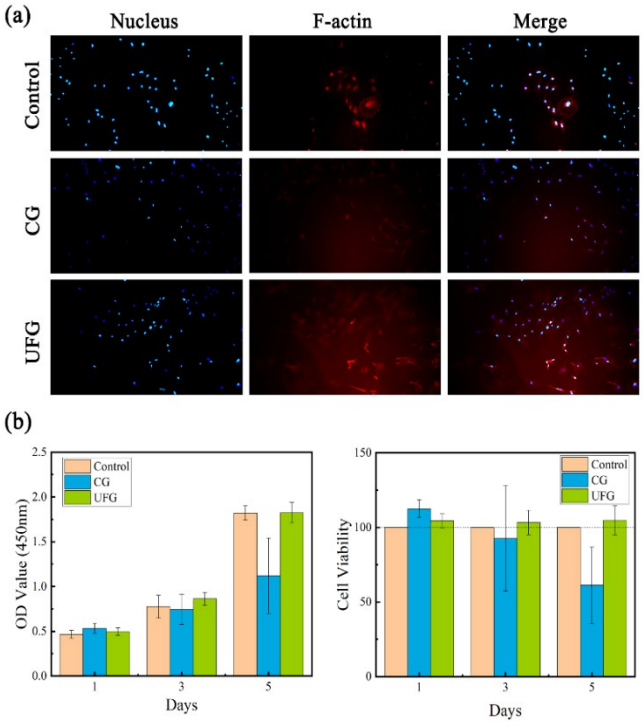

Figure 2. Cytoskeleton staining results (a) and cytotoxicity experiment (CCK-8) results (b).

Figure 3 shows the ALP staining of MC3T3-E1 cells. The results reveal that cells in the UFG composite group exhibited significantly higher ALP secretion compared to the control group. Additionally, they displayed more extensive and denser areas of darker staining [9]. While the ALP concentration in the CG group was elevated compared to the control group, the proportion of darker areas was noticeably lower than that observed in the UFG group. This implies that lower Mg^{2+} ion concentrations play a role in facilitating ALP secretion and mineralization in MC3TE-E1 cells.

Furthermore, western blot analysis was conducted to assess osteogenic differentiation ability on day 7, as depicted in Figure 4. In comparison to the CG composite and control groups, the UFG composite group exhibited higher production levels of osteogenesis-related proteins, including BMP-2, Col-I, OPN, and Runx2. Quantitative analysis (depicted in Figure 4(a)) shows that MC3T3-E1s treated with CG composite extracts produced more OPN and Runx2 compared to control group, but a lower production level of BMP-2, Col-I. On the other hands, the MC3T3-E1s treated with UFG composite demonstrated a consistently higher expression than the control group. These findings indicate that lower Mg^{2+} ion concentrations exert distinct positive effects on osteoblast proliferation, differentiation, and bone matrix deposition.

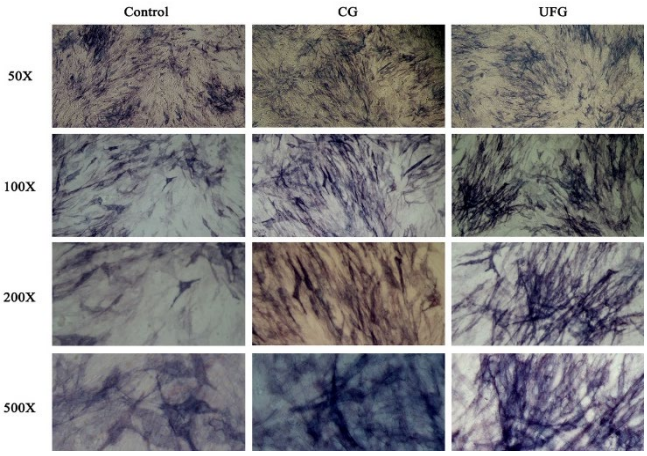

Figure 3. Staining photographs showing the ALP staining of MC3T3-E1s cultured for 7 days.

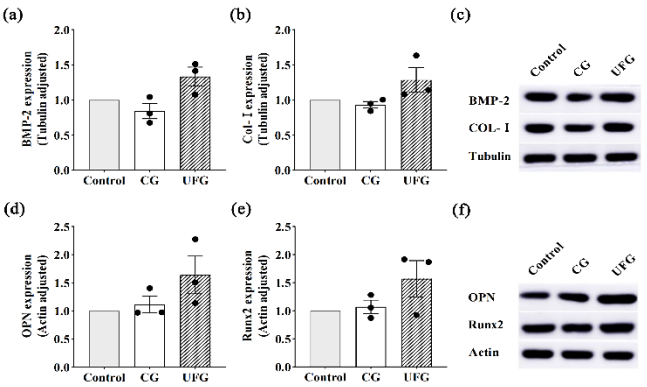

Figure 4. Western blot analysis of BMP-2, Col-I, OPN and Runx2 on day 7. (a) quantitative analysis of BMP-2 expression; (b) quantitative analysis of Col-I expression; (c) western blot image for BMP-2 expression; (d) quantitative analysis of OPN expression; (e) quantitative analysis of Runx2 expression; (f) western blot image for OPN and Runx2 expression.

For determining the in vivo biodegradation and bone regeneration capacity, CG and UFG composites were implanted in rat femoral condyle. The 3D reconstruction results of the two material implants after 12 weeks post-implantation is shown in Figure 5(a) and Figure 5(b). As shown in Figure 5(c), the volume of the CG composite was approximately 10.7 mm^3, a reduction of approximately 15.4% compared to the original state (0 Week). In contrast, the volume of the UFG composite was 12.18 mm^3, a reduction of only 3.2% relative to the original volume. The corrosion resistance of the UFG composite is much higher than that of the CG composite. Meanwhile, from the reconstruction results, the surface of UFG composites shows the characteristics of uniform corrosion without obvious pitting. However, obvious pitting corrosion can be observed for CG composites. The quantitative analysis of the micro-CT reconstruction images of newborn trabecular bone depicts bone mineral density (BMD), bone volume/tissue volume (BV/TV,), trabecular bone thickness (Tb. Th), and trabecular numbers (Tb. N) in Figure 5(d). As compared with CG composite, the osseous tissues formed in UFG composite implants are featured with higher bone parameters. It validates that the regenerated bone tissue embraced in UFG composite implant is more abundant in terms of morphology and morphometry.

Histological examinations of the adjacent bone tissue are presented in Figure 5(e). Histological analysis using H&E staining of both UFG and CG composites revealed no apparent signs of inflammatory reactions or immune rejection, indicating excellent in vivo biocompatibility. Due to the enrichment of Calcimine (Ca) in the bone matrix, the Von Kossa staining can be a good indicator of bone tissue formation because of the Ca deposition in the bone matrix. It can also be observed that the newly formed collagenous tissue (yellow-brown area around the implants) was more obvious in UFG group, which indicated the improved osteogenic ability. Furthermore, the polarization of macrophages from inflammatory (M1) to anti-inflammatory (M2) is crucial for enhancing osteogenic properties during the bone remodeling process. From the staining results in Figure 5(e), significantly low numbers of M1-polarized macrophages were detected around the implants of both materials. This suggests that a significant inflammatory response is not occurring around either UFG and CG implants. In contrast, M2-polarised macrophages were more pronounced in the tissue surrounding the UFG implant [10]. This implies that UFG composites exhibit a more substantial promotion of immunomodulation, angiogenesis, bone remodeling, and repair.

Previous research demonstrates that Mg^{2+} can upregulate anti-inflammatory cytokines through the inhibition of nuclear factor kappa-B (NF-Kb) and toll-like receptor (TLR) pathways, leading to increased expression of BMP-2, transforming growth factor beta (TGF-β), vascular endothelial growth factor (VEGF), and osteoblast mineralization [11]. Nonetheless, the higher corrosion rate and increased release of Mg^{2+} from CG composites led to the inhibition of BMP-2 expression when compared to UFG composites [9]. This suggests that CG composites are less effective in promoting bone repair compared to UFG composites, which aligns with the findings from the CT scans (Figure 5(d)). Reduced pitting and lower degradation rates contribute to the regulation of Mg^{2+} ion concentration around the implant. This facilitates enhanced expression of genes associated with bone formation when optimal Mg ion concentrations are maintained. Thus, the UFG materials exhibit an enhanced capacity to promote bone growth.

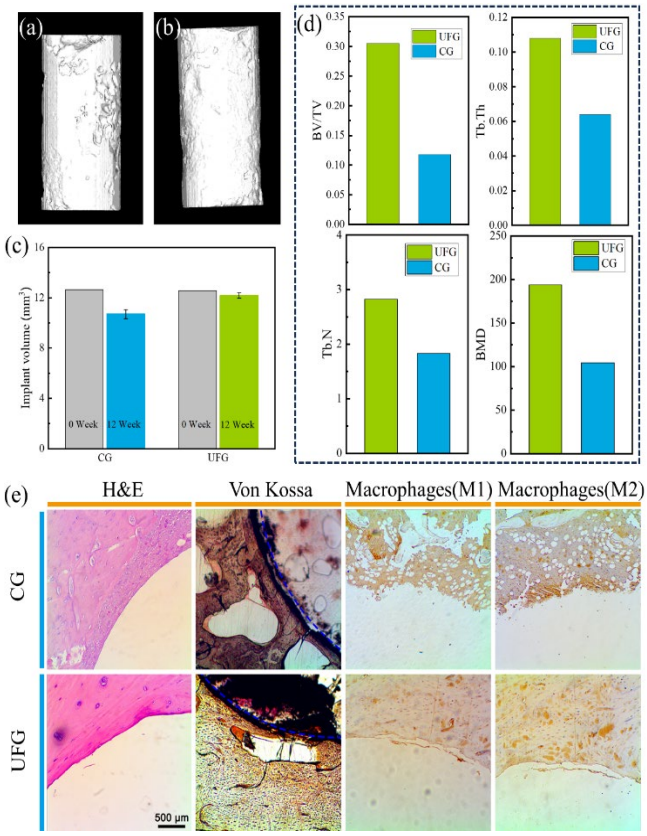

Figure 5. 3D reconstruction result of CG (a) and UFG (b), degradation volume (c), quantitative analysis of BMD, BV/TV, Tb. Th and Tb. N (d), and histological studies of H&E, Von Kossa, and macrophages polarization (e).

4. Conclusion

In summary, the Mg-1Zn-0.2Ca-1.0MgO composite with ultra-fine grained (UFG) structure showed a higher corrosion resistance and lower release of Mg^{2+}. Less pitting and lower degradation rates help to control the concentration of Mg ions around the implant. Allows for better expression of bone-contributing genes in the presence of appropriate concentrations of Mg ions. Improved bone-enhancing ability of UFG materials.

Declarations

Ethics approval: The animal study was reviewed and approved by the Tianjin Hospital of Integrated Chinese and Western Medicine.

Consent for publication: Not applicable.

Availability of data and materials: The original contributions presented in the study are included in the article, further inquiries can be directed to the corresponding authors.

Competing interests: The authors declare that they have no known competing financial interests or personal relationships that could have appeared to influence the work reported in this paper.

Acknowledgment

Shuquan Zhang received grants from the Science and technology project of Tianjin Municipal Health Commission (No. TJWJ2023MS023), the Natural Science Foundation of Tianjin city of China (No. 21JCYBJC

00490), and the crosswise tasks of Tianjin Hospital of Integrated Chinese and Western Medicine (No. HXKY2020-0825).

Minfang Chen received a grant from the National Natural Science Foundation of China (No. 52201301).

Shaoyuan Lyu received a grant from the National Natural Science Foundation of China (No. 52171241).

Shaoyuan Lyu received grants from the Natural Science Foundation of Tianjin city of China (No. 22JCQNJC00750).

Jiangtao Feng received grants from the Natural Science Foundation of Tianjin city of China (No. 21JCQNJC01040), and the project of Tianjin Municipal Health Commission (No. 2023168).

This funding has been instrumental in supporting the research work and its publication, hence it is essential to accurately reflect it in the final article.

References

[1] M. P. Staiger, A. M. Pietak, J. Huadmai, and G. Dias, "Magnesium and its alloys as orthopedic biomaterials: a review," *Biomaterials,* vol. 27, no. 9, pp. 1728-1734, 2006.

[2] N. Singh, U. Batra, K. Kumar, N. Ahuja, and A. Mahapatro, "Progress in bioactive surface coatings on biodegradable Mg alloys: A critical review towards clinical translation," *Bioact Mater,* vol. 19, pp. 717-757, 2023.

[3] Y. Chen, Z. Xu, C. Smith, and J. Sankar, "Recent advances on the development of magnesium alloys for biodegradable implants," *Acta Biomater,* vol. 10, no. 11, pp. 4561-4573, 2014.

[4] S. Y. N. Wang, H. Shi, Y. Song, H. Sun, Q. Wang, L. Tan, and S. Guo, "Magnesium alloys for orthopedic applications: A review on the mechanisms driving bone healing," *Journal of Magnesium and Alloys,* vol. 10, no. 12, pp. 3327-3353, 2022.

[5] Y. H. Chang, C. C. Tseng, C. Y. Chao, C. H. Chen, S. Y. Lin, and J. K. Du, "Mg-Zn-Ca alloys for hemostasis clips for vessel ligation: In Vitro and In Vivo studies of their degradation and response," *Materials (Basel),* vol. 13, no. 13, 2020.

[6] F. Feyerabend, F. Witte, M. Kammal, and R. Willumeit, "Unphysiologically high magnesium concentrations support chondrocyte proliferation and redifferentiation," *Tissue engineering*, vol. 12, no. 12, pp. 3545-3556, 2006.

[7] Z. Y. Fan, Y. B. Zuo, and B. Jiang, "A new technology for treating liquid metals with intensive melt shearing," *Materials Science Forum,* vol. 690, pp. 141-144, 2011.

[8] M. D. S. Thanka Rajan, A. Arockiarajan, "In vitro assessment of corrosion resistance and biocompatibility of tantalum-niobium oxide surface-functionalized Mg alloy," *Materials Chemistry and Physics,* vol. 301, p. 127560, 2023.

[9] D. Zhao, K. Yu, T. Sun, X. Jing, Y. Wan, K. Chem, H. Gao, Y. Wang, L. Chen, X. Guo, and Q. Wei, "Material–Structure–Function integrated additive manufacturing of degradable metallic bone implants for load-bearing applications," *Advanced Functional Materials,* vol. 33, no. 16, p. 2213128, 2023.

[10] Y. Wang, Y. Fan, and H. Liu, "Macrophage polarization in response to biomaterials for vascularization," Annals *of Biomedical Engineering*, vol. 49, no. 9, pp. 1992-2005, 2021.

[11] M. Wang, Y. Yu, K. Dai, Z. Ma, Y. Liu, J. Wang, and C. Liu, "Improved osteogenesis and angiogenesis of magnesium-doped calcium phosphate cement via macrophage immunomodulation," *Biomaterials Science,* vol. 4, no. 11, pp. 1574-1583, 2016.